



Sharif University of Technology
Scientia Iranica
Transactions B: Mechanical Engineering
<http://scientiairanica.sharif.edu>



Numerical analysis of the application of different lattice designs and materials for reciprocating engine connecting rods

M.G. Gok^{a,*} and O. Cihan^b

a. *Department of Material Science and Engineering, Hakkari University, Hakkari, Turkey.*

b. *Department of Mechanical Engineering, Hakkari University, Hakkari, Turkey.*

Received 15 November 2021; received in revised form 25 January 2022; accepted 16 May 2022

KEYWORDS

Weight reduction;
 Lattice design;
 Connecting rod;
 Mechanical properties;
 Finite element;
 Fatigue analysis.

Abstract. Nowadays, the application of lattice structure designs in metallic parts to produce lightweight systems has gained higher importance owing to advances in additive manufacturing technology. In the meanwhile, vehicle manufacturers are constantly looking for new ways to reduce the weight resulting from the depletion of fossil fuels, demand for vehicles with higher performance, global warming, and increasingly stringent emission standards. Different lattice designs were made in the connecting rods in this study to reduce the weight of the internal combustion engine. Four different 2.5D lattice designs, i.e., hexagonal, octagonal, square, and triangular designs, were created on the reference connecting rod body. The dimensions of the lattice designs were $10 \times 10 \times 12$ mm with the wall thickness of 1.5 mm. The fatigue behavior of the connecting rods as well as mechanical properties under static conditions were analyzed using the finite element approach. Three different materials were used in AISI 4140, Inconel 718, and Ti6Al4V analyses. It was found that a 15.75% weight reduction was made possible in the case of connecting rod owing to the lattice designs, and the maximum stress value was below the yield stresses of the materials. According to the findings, connecting rods with lattice design yielded satisfactory safety factor values.

© 2022 Sharif University of Technology. All rights reserved.

1. Introduction

Application of lightweight materials in air and land vehicles is an important method for performance improvement [1–3]. Therefore, such improvement is closely related to advances in materials science and manufacturing techniques. New manufacturing tech-

niques facilitate lightweight designs in engine materials, thus making it possible to significantly reduce the engine mass, compared to the conventional designs. As a result, a significant contribution is made to reduce the overall weight of vehicles [4]. Nowadays, considering the serious environmental concerns such as global warming and the relevant strict policies, vehicle manufacturers who put a great deal of effort to reduce fuel consumption are constantly looking for ways to reduce the weight even more [5]. For a more comprehensive understanding of the relationship between the fuel economy and mass, the following example is given. If the weight of a 1500 kg vehicle is reduced by only 150 kg (or 10%), a reduction in the fuel consumption

*. *Corresponding author.*

E-mail addresses: m.guvengok@hakkari.edu.tr,
mggok@itu.edu.tr (M.G. Gok); omercihan@hakkari.edu.tr,
ocihan@itu.edu.tr (O. Cihan)

would be approximately 7% [6]. Moreover, even the smallest detail of designs involved in reducing the weight of the mechanical parts of the engine affects the total fuel consumption and life of the parts [7].

A suggested option to make lightweight designs is to use lattice structures in metallic engine parts [8] that enjoy several advantages such as high strength and low weight, to name a few [9]. Moreover, these lattice structures can considerably eliminate material wastes [10]. At the same time, it is possible to reduce the weight of the materials without a significant reduction of their mechanical properties. Thanks to the latest advances in additive manufacturing technology, it is possible to produce very precise lattice structures at high resolutions. Given that additive manufacturing is a near net shape manufacturing technology, post-production processes are not required. In addition, owing to this environmentally-friendly technology, the properties and qualities of the materials are higher than those of the traditional methods [11–14]. Flores et al. [15] demonstrated that the application of lattice designs to the production of lightweight parts with additive manufacturing techniques would decrease the unit cost, manufacturing time, and weight by 70.6%, 71.1%, and 54.3%, respectively, compared to those in the traditional solid infill designs.

Connecting rods are one of the important parts of reciprocating engines [16,17]. They are mechanical parts that transmit the variable axial movement in the form of the push and pull of the piston to the crankshaft [18]. Consequently, the connecting rod converts the reciprocating motion of the piston into the rotational motion of the crankshaft [19,20]. With the movement of burnt gases and inertial components in the engine, pressure will be imposed on the connecting rod, thus creating compression and tensile stress, respectively [21]. Reciprocating engines have at least one connecting rod depending on the number of cylinders [22]. Until today, many studies have been carried out on the connecting rods such as stress, deformation, fatigue, and use of different materials. The connecting rod material is usually made of low alloy steel such as AISI 4140. Saravanan et al. [23] analyzed the existing connecting rod materials, i.e., AISI 4140 steel and AL S355 (aluminum) cast alloy using Ansys software. The reason behind using the AL S355 casting alloy is its high strength and much less density than that of steel. However, due to the poor mechanical properties of Al 355 alloy, compared to AISI 4140, it is not suitable for high-compression-ratio engines in which connecting rods are made of AISI 4140 material are used. Instead of AISI 4140 steel, many other materials such as titanium alloy, aluminum alloy, and glass fiber composite can be used to reduce weight in the connecting rod [24,25]. However, considering the actual load produced by the

piston resulting from combustion and fatigue life under these load conditions, one may conclude that the application of alternative materials is not possible in most cases. Instead, titanium alloys such as Ti6Al4V are used in the mechanical parts due to their light-weight and high-strength properties [26]. Ajayi-Oluwaseun et al. [27] evaluated the effect of shape optimization on Ti6Al4V as a connecting rod material in a 500 cc engine. They reported a 11.7% reduction in weight, lower deformation, and notable stress distribution in the optimized model. Loga and Ku [28] carried out a design and fatigue analysis using c70s6by steel (with relatively poor mechanical properties) and titanium alloys in the Ansys software. Titanium alloy connecting rod yielded better results than steel one in terms of static mechanical and fatigue life properties. Lattice structures in different designs are generally used to reduce weight and increase strength in the connecting rods. Rosso et al. [29] tested the lattice structure on the whole body of the connecting rods and pointed out the possibility of using lattice design in the connecting rods for some applications. Shanmugasundar et al. [30] designed a different structure by drilling five circular holes on the body of a connecting rod. They reported an about 3.5% reduction in the weight of the connecting rod with no deterioration in its mechanical properties.

The main objective of this study is to reduce the weight of the connecting rods using different lattice designs and to numerically evaluate the effect of these designs on their mechanical properties. Despite the limited studies on the application and analysis of 3D lattice designs in the connecting rods, to the best of the author's knowledge, no study on the application and analysis of 2.5D lattice designs in the connecting rods was found in the literature. The reference connecting rod design belonged to the Antor 3 LD 510 single-cylinder diesel engine. Four different 2.5D lattice designs in hexagonal, octagonal, square, and triangular forms were made in this reference and implemented on the connecting rod body. The dimensions of the lattice designs were $10 \times 10 \times 12$ mm with a wall thickness of 1.5 mm. In the analysis, three different materials namely AISI 4140, Inconel 718, and Ti6Al4V were used as the connecting rods in some engines that were also suitable for production based on the additive manufacturing methods. The load on the connecting rod was determined based on the experimental setup to which the Antor 3 LD 510 engine was connected. As a result, it can be stated that lattice designs can be used in the connecting rods and consequently, these designs can significantly reduce the weight. As stated earlier, to the best of the authors' knowledge, no study has been found on this issue in the literature, and this is the main reason why this study will be an important resource for both vehicle manufacturers and researchers working on this subject.

(part no 4). The geometry of the original connecting rod was compatible with that of the connecting rod used in the Antor 3 LD 510 single-cylinder diesel engine, and the maximum in-cylinder pressure values for application were obtained in this study. The length, rod thickness, small end diameter, and big end diameter of the original connecting rod were 145 mm, 12 mm, 15 mm, and 48 mm, respectively. The 2.5D lattice designs in the connecting rod were made using Creo Parametric 7.02 software (Student Edition). As observed in Figure 1, the dimensions of all lattices are $10 \times 10 \times 12$ mm with a wall thickness of 1.5 mm.

2.2. Meshing and material properties

The designed connecting rods were exported to the ANSYS 2020 software. In order to obtain more accurate results in the finite element numerical modeling study of the connecting rods, the average mesh quality value was suggested to be 0.8 and above. To achieve this value, tetrahedron meshes were utilized. The connecting rod was divided into three parts, and different mesh methods were applied. Since each design contains lattices with different geometries, the mesh quality should be adjusted with the “patch independent” option in the body of the connecting rod and

cap. Table 1 presents the meshing conditions and obtained. Figure 2(b) shows the finite element model of the connecting rod after the meshing process. In this study, three different materials were selected to be used in the connecting rods, and their designs were analyzed based on these materials. The first material is AISI 4140 steel which is currently used as the connecting rod material of many internal combustion engines. It is also used in the connecting rod of the Antor 3 LD 510 model single cylinder diesel engine based on which the in-cylinder pressure values can be obtained (Figure 3(a)). The second material used in the connecting rod is Inconel 718 alloy, which is characterized by high-strength properties and resistance at elevated temperatures. Although this feature is of special importance in aerospace applications, it has not been studied as the connecting rod material to date. In this respect, the current study aims to analyze this material for the first time. The third material used in the connecting rods is Ti6Al4V alloy. Due to its low density (4.41 g/cm^3), it is used as a connecting rod material in the internal combustion engines of automotive and aircraft industries.

Since the connecting rods with lattice design in this study can be appropriately produced through

Table 1. Meshing parameters of finite element.

Design	Part no	Algorithm	Method	Element size (mm)		Nodes	Elements
				Max.	Min.		
Reference				3	1.5	163340	110520
Hexagonal				4	2	164722	107142
Octagonal	1	Patch independent	Tetrahedrons	4.5	2	193566	127187
Square				3.5	2	190770	126227
Triangle				3	2	202560	132219
For all designs	2			5	3	21559	13765
	3, 4	Automatic	Tetrahedrons+Hexahedrons			35377	9233

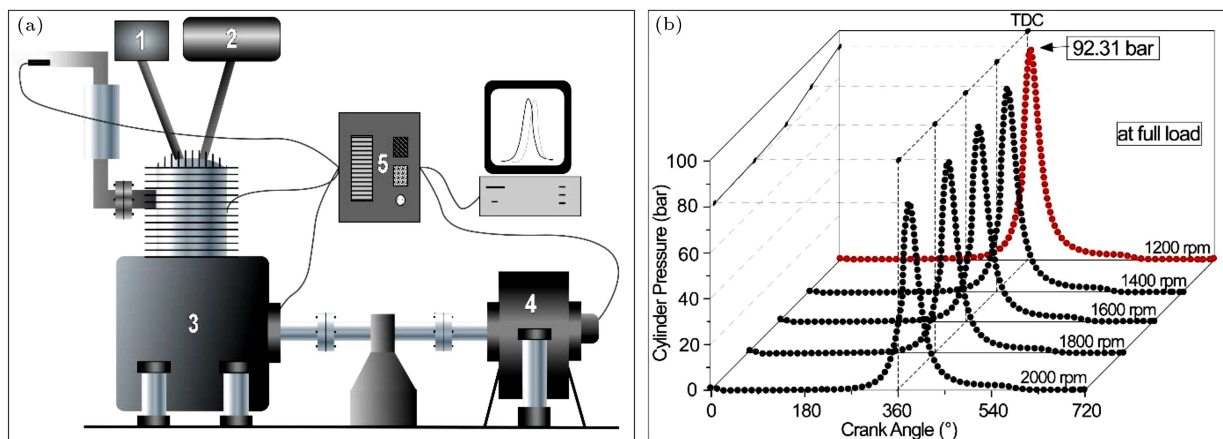


Figure 3. (a) Schematic explanation of engine setup to obtain load on the connecting rod: 1) air filter, 2) fuel tank, 3) engine, 4) dynamometer, and 5) control panel. (b) Cylinder pressure graphs at full load and different engine speeds.

the additive manufacturing methods, their mechanical properties produced by the additive manufacturing methods given in the literature were taken into consideration. Damon et al. [31] produced low-alloy AISI 4140 steel using the selected laser melting technique. They calculated the maximum young modulus, yield strength, ultimate strength, and ductility as 208 GPa, 1290 MPa, 1325 MPa, and 7.2%, respectively. In another study carried out by Wang et al. [32], the values of the young modulus, yield strength, ultimate tensile strength, and ductility of Inconel 718 (IN718) alloy produced by selective laser melting + heat treatment process were measured as 201 GPa, 1161 MPa, 1358 MPa, and 22%, respectively. In the case of Ti6Al4V production by selective laser melting + heat treatment process, the values of the maximum young modulus, yield strength, ultimate tensile strength, and ductility were measured as 115.5 GPa, 1118 MPa, 1223 MPa, and 14.06%, respectively [33].

2.3. Load on connecting rod

The load imposed on the connecting rod is the most important factor that determines the mechanical behavior of the connecting rod [34]. In this respect, determining the actual load that affects the connecting rod in the numerical modeling studies is essential to obtain accurate results. In this study, an experimental setup characterized by Antor 3 LD 510 model direct injection diesel engine was used to obtain accurate load on the designed connecting rod. The test engine is commonly used for research purposes in many studies today [35,36]. This single-cylinder, four-stroke, and

direct injection diesel engine was controlled by electric dynamometer, and the experiments were conducted at full load and engine speeds ranging from 1200 to 2000 rpm to create harsh conditions for the connecting rod. The cylinder volume, bore \times stroke, compression ratio, maximum power, and maximum torque of the engine were measured as 510 cm³, 85 \times 90 mm, 17.5:1, 8.8@3000 kW, and 32.8@2000 Nm, respectively. Schematic explanation of the engine experimental setup is given in Figure 3(a).

Figure 3(b) illustrates the graph of pressure changes versus the crankshaft angle at full load and different engine speeds according to which the maximum cylinder pressure is obtained as 92.31 bar at the engine speed of 1200 rpm. This gas pressure value was then converted into newton units using Eq. (2). In order to calculate the net force (F) imposed on the connecting rod (Eq. (1)), the forces caused by the gas pressure (Eq. (2)), inertia of the connecting rod and reciprocating mass (Eq. (3)), and friction of the piston rings and of the piston (Eq. (4)) should be calculated. As the weight of the connecting rod changes in each material and design, the inertia force also changes. Therefore, the maximum net force imposed on the connecting rod is calculated for each material and design, and the obtained results are given in Table 2.

$$F = F_{\text{gas}} + F_{\text{inertia}} - F_{\text{friction}}, \quad (1)$$

$$F_{\text{gas}} = \frac{\pi * d^2}{4} * P_e. \quad (2)$$

Here, P_e and d represent the explosion pressure and

Table 2. Connecting rod materials and mechanical properties belonging these materials produced by additive manufacturing process, weights of different designs, and maximum net forces acting on connecting rod for each design.

Material	Design	Weight (g)	Max. force (N)	Young's modulus (GPa)	Yield strength (MPa)	UTS (MPa)	Poisson ratio
AISI 4140	Reference	906.92	53077				
	Hexagonal	772.48	53045				
	Octagonal	775.62	53046	210	1540	2073	0.29
	Square	764.11	53043				
	Triangle	802.14	53052				
Inconel 718	Reference	949.56	53087				
	Hexagonal	808.80	53053				
	Octagonal	812.08	53054	201	1161	1358	0.3
	Square	800.04	53051				
	Triangle	839.85	53061				
Ti6Al4V	Reference	508.88	52982				
	Hexagonal	433.45	52964				
	Octagonal	435.21	52965	115.5	1118	1223	0.32
	Square	428.75	52963				
	Triangle	450.09	52968				

bore diameter, respectively.

$$F_{\text{inertia}} = M * \omega^2 * r * \left(\cos \theta + r * \frac{\cos \theta}{I} \right), \quad (3)$$

where M is the mass of (*piston and rings + piston pin + 1/3rd of the connecting rod*), ω the angular speed (rad/s), r the crank radius (mm), l the length of the connecting rod (mm), and θ the crank angle.

$$F_{\text{friction}} = h * \pi * d * i * P_r * \mu, \quad (4)$$

where h stands for the axial width of rings, i the number of seals, P_r the pressure of seals, and μ the friction coefficient.

2.4. Boundary conditions and analysis

As observed in Figure 2(c), the designed connecting rods were fixed from the big end bearing surfaces to perform numerical analysis. Of note, the forces generated during the engine operation are affected by the weight of the connecting rod. In this regard, the maximum net compression forces given in Table 2 were applied to the small end bearing surface of the connecting rod. In the numerical analysis, the bonded contact was used for all parts of the connecting rod. During the engine operation, the ambient temperature of the connecting rod was determined to be 95°C; therefore, the ambient temperature was set as 95°C during the analysis. These boundary conditions were imposed to simulate the effects of different materials and designs on the mechanical properties such as stress, deformation, strain, and fatigue that occur in the connecting rod during the actual engine operation. In this situation, the weight savings achieved by different designs were first evaluated. Then, nonlinear static structural and fatigue analyses were carried out in ANSYS software. The values of maximum deformation (mm), maximum stresses (equivalent von-mises (MPa)), fatigue lives, safety factors, and damage conditions according the Goodman stress theory and fully reversed loading conditions were calculated at the maximum applied loads. In fact, thermal fatigue is an important factor in the operability of metallic materials at high temperatures [37]. However, the operating temperature of the connecting rods in the internal combustion engines is around 95°C, and the temperature difference between regions is not very high. In addition, the connecting rods are not exposed to cycling thermal effect during operation. This is the reason why this study neglected the thermal fatigue in the connecting rods with lattice designs.

3. Results and discussions

3.1. The effect of connecting rod designs on weight reduction

Creating lattice designs on the body of the connecting rod would save the amounts of used materials and,

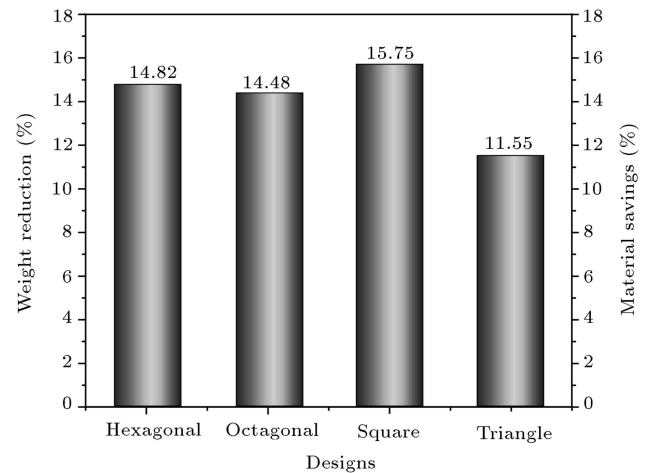


Figure 4. The percentage change in weight of the designs relative to the reference design of the connecting rod.

more importantly, reduce its weight significantly. Table 2 lists the values of the changes in weights (in grams) according to designs and materials. Figure 4 shows the weight changes (in percentage) in the designs relative to the reference material (without lattice structure). Accordingly, the highest weight reduction (15.75%) was observed in the “square” design, while the least weight loss (11.55%) was in the “triangle” design, mainly because in the given dimensions (Figure 1), the tightest pecked structure was formed in the triangular design. Based on this finding, it can be concluded that lattice designs can significantly cause weight loss in the connecting rod. Given that there are four connecting rods in the engine of a normal passenger vehicle, there will be considerable savings in terms of fuel economy. In addition, there was considerable material saving at the same rate as the weight reduction percentage. However, the effect of such a weight reduction on the mechanical properties should also be taken into consideration (see Section 3.3). As a natural consequence of weight reduction caused by lattice designs on the connecting rod body, the mechanical properties are likely to be weakened due to the locally reduced cross-sectional area of the connecting rod body. At this point, the maximum equivalent stress value that takes place in the connecting rod under maximum load transmitted from the piston to the connecting rod must be lower than the yield value of the material of the connecting rod. It is also necessary to achieve certain minimum values for the stress factor of safety and fatigue life discussed in Sections 3.2 and 3.3.

3.2. Static structural analysis

The maximum stress and deformation values obtained under maximum load in the static-structural modeling of the connecting rods were also analyzed. As observed in Figure 5(a), the equivalent (Von-Mises) stress values

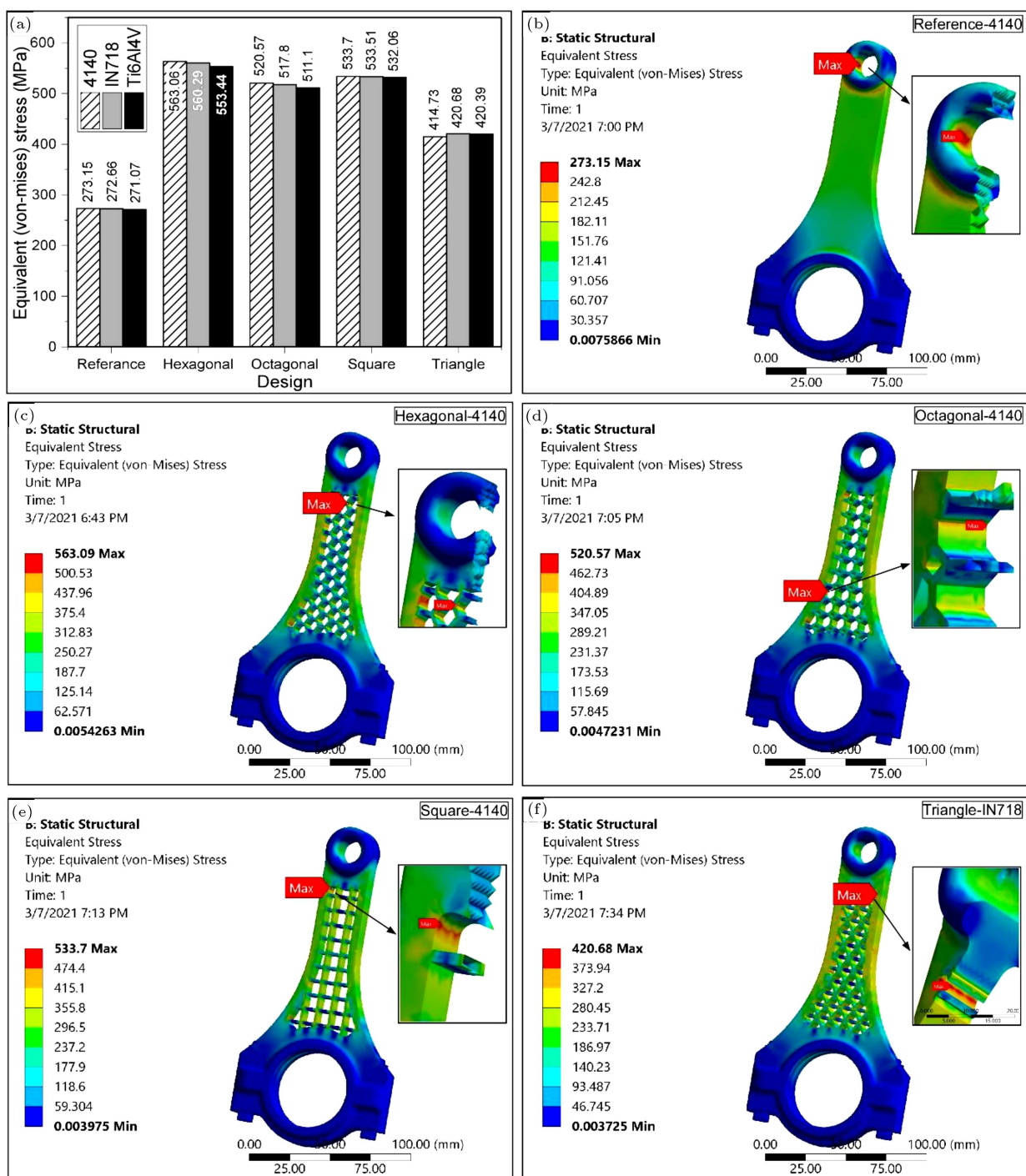


Figure 5. Static analysis results of connecting rods having different designs and materials: (a) Column graph showing maximum Von-Mises stress. Stress distributions on (b) reference-4140, (c) hexagonal-4140, (d) octagonal-4140, (e) square-4140, and (f) triangle-IN718.

for each design were close to each other, mainly due to the close mechanical properties of 4140, IN718, and Ti6Al4V. As expected, the minimum tensile values ranging from 271.07 to 273.15 MPa were attributed to the reference designs. The maximum stress values in the connecting rods with lattice designs of hexagonal, octagonal, and square forms varied between 511.1 and

563.06 MPa. However, the connecting rods with a triangular lattice design had lower maximum tensile values (ranging from 414.73 to 420.68 MPa) because in the triangle design, the applied load was transferred equally along the sides of the triangle to the non-lattice-formed part of the connecting rod. However, in other designs, the applied load was more difficult to transmit

Table 3. Safety factors for static conditions and fatigue conditions as well as fatigue life.

Material	Design	Safety factor for static conditions	Fatigue life (cycles $\times 10^6$)	Safety factor for fatigue conditions
AISI 4140	Reference	5.64	> 1000	2.37
	Hexagonal	2.74	> 1000	1.15
	Octagonal	2.96	> 1000	1.24
	Square	2.89	> 1000	1.21
	Triangle	3.71	> 1000	1.56
Inconel 718	Reference	4.26	> 1000	2.27
	Hexagonal	2.07	> 1000	1.11
	Octagonal	2.24	> 1000	1.20
	Square	2.18	> 1000	1.16
	Triangle	2.76	> 1000	1.47
Ti6Al4V	Reference	4.12	> 1000	1.77
	Hexagonal	2.02	= 5.84	0.87
	Octagonal	2.19	= 51.8	0.94
	Square	2.10	= 15.6	0.90
	Triangle	2.66	> 1000	1.14

due to the vertical or wide-angle joints of the lattice walls. The maximum equivalent Von-Mises stress value must be smaller than the yield strength ($\sigma_{0.2}$) value of that material to avoid permanent deformation in the material. In other words, under static conditions, the value of the safety factor (the ratio of the yield strength of the material to the stress value measured in design) must be greater than 1. While reviewing the literature [31–33], it was found that the yield strength values of AISI 4140, IN718, and Ti6Al4V (1540, 1161, and 1118 MPa, respectively) materials produced by additive manufacturing methods were higher than the maximum obtained Von-Mises stress values. According to Table 3, the safety factor of all lattice designs under static loading conditions is between 2.02 and 3.71. These values are higher than the static safety factor determined by Pan and Zhang as 1.77 for the standard connecting rod made of T6-7075 material [38]. Consequently, it can be concluded that the connecting rods with designed lattice structures remain rigid without permanent deformation under the maximum load resulting from the combustion chamber pressure of the engine, hence safe to be used as a connecting rod. However, determining how these designs would respond mechanically to cyclic load application and how many cycles their lifetime would be under this cyclic load is of importance. These fatigue-related facts will be discussed in Section 3.3. Figure 5(b)–(f) shows the stress distribution of the connecting rod materials based on which the maximum Von-Mises stress can be obtained for each design. According to Figure 5(b),

the maximum stress occurs in the piston pin region of the reference connecting rod. However, in the lattice structured designs, the maximum stresses are found in the lattice structure regions and specifically concentrated in the joining corners of the lattice walls (see focused figures in Figure 5(b)–(f)), mainly because the cross-sectional area of the lattice walls is narrower than that of the main structure, and the direction of the stress flowing linearly along the lattice walls should suddenly change at the joining corners. Therefore, higher stress concentrations are commonly observed in these regions. It is possible to reduce the stresses in these areas by chamfering the joining corners of the lattice walls. In this study, the stresses imposed on the designed connecting rods were not higher than the yield strength of the materials, hence no need for optimization such as chamfering in the designs.

As can be seen in Figure 6(a), the deformation value of the designed connecting rods varies from 0.08853 to 0.33919 mm. As expected, the number of deformations was minimal in the reference connecting rods without lattice structure. Upon evaluating the materials, it was observed that maximum deformations occurred in designs with Ti6Al4V material. Accordingly, the young modulus value of Ti6Al4V material produced by additive manufacturing method (115.5 GPa) was lower than 4140 (210 GPa) and IN718 (201 GPa) [31–33]. Therefore, the deformation values of AISI 4140 and IN718 were approximately close to each other in the design of each connecting rod. The deformation distribution of the Ti6Al4V

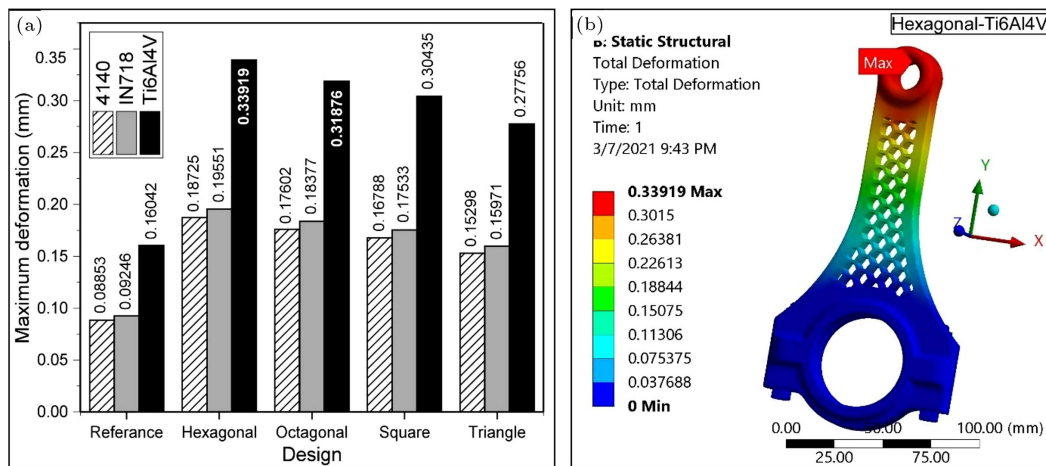


Figure 6. (a) Maximum deformation graph and (b) deformation distributions on the hexagonal 4140 connecting rod.

material in the connecting rod with the hexagonal lattice design is presented in Figure 6(b) where the highest deformation (0.33919 mm) can be obtained since in the connecting rod with a hexagonal design, the hexagonal geometry behaves like a spring and is, thus, deformed more elastically. According to the findings, maximum deformation occurred at the end of the pin associated with the piston. Since the area in the pressure distribution was very small in all other designs, the maximum deformation was observed in the same place.

3.3. Fatigue analysis

Under static conditions, the safety factors of the connecting rods with lattice designs were above two, which is more than 1, thus meeting the static requirement. However, during the engine operation, the piston has continuously reciprocating movements and a cycling stress occurs in the connecting rod. As a result, damages caused by long-term periodic repetition of this stress are likely to happen; however, they do not harm the connecting rod under static conditions. This phenomenon is referred to as fatigue. In the fatigue analysis, Goodman equation was used to determine the cycling life of the connecting rod designs and solve the fatigue safety factor. As observed in Table 3, the cycling fatigue life of all connecting rods was above 1×10^9 , except for the hexagonal, octagonal, and square designs made of Ti6Al4V material. From this point of view, it can be stated that all connecting rods, except for the hexagonal, octagonal, and square designs made of Ti6Al4V material, can operate for at least 13,889 hours at 1200 rpm where the maximum in-cylinder pressure is imposed at maximum load. While assessing the fatigue life of the connecting rod made under full load and maximum engine pressure conditions, it was found that the rod must withstand at least 10×10^6 cycles [39]. Therefore, designs with a cycling fatigue life of more than 10×10^6 can be claimed to have infinite

lifetimes. In the present study, the cycling fatigue lives of hexagonal, octagonal, and square designs of Ti6Al4V connecting rods were determined as 5.84×10^6 , 51.8×10^6 , and 15.6×10^6 , respectively. Hence, these connecting rods can work up to 81.1, 719.4, and 216.7 hours, respectively, at full load and 1200 rpm.

While the fatigue analysis results were evaluated in terms of the cycling safety factor, it was found that the reference connecting rods had the highest minimum cycling safety factor values varying from 1.77 to 2.37. It was also reported that the minimum cycling safety factor value was between 1.14 and 1.56 in all designs except for the connecting rod with Ti6Al4V material with hexagonal, octagonal, and square designs. To be specific, these designs with the minimum cycling safety factor more than “1” have no difficulty in their reliability in terms of fatigue since the cycling safety factor for connecting rods should be between “1” and “2”. Otherwise, a very high safety factor was known to lead to negative consequences such as weight, excessive material use, and design difficulties. While examining the cycling safety factor values of the connecting rods with Ti6Al4V material with hexagonal, octagonal, and square designs, it was found that they remained below “1” in accordance with their cycling fatigue life values, mainly due to the relatively low fatigue strength of the Ti6Al4V material. The risk of failure is quite high in the hexagonal design, especially for this material. Figure 7(a) and (c) shows the safety factor distribution of the connecting rod designs with the lowest fatigue life. As expected, the regions with the minimum cycling safety factor were the ones with the most intense static stresses discussed in Section 3.2. This condition holds for all other designs (as seen in Figure 7(d)). The overall cycling safety factor of the connecting rod is likely to be improved by either increasing the thickness of the lattice wall or chamfering at the joining corners of the lattice walls. However, the negative effect of these procedures on the weight should also be taken

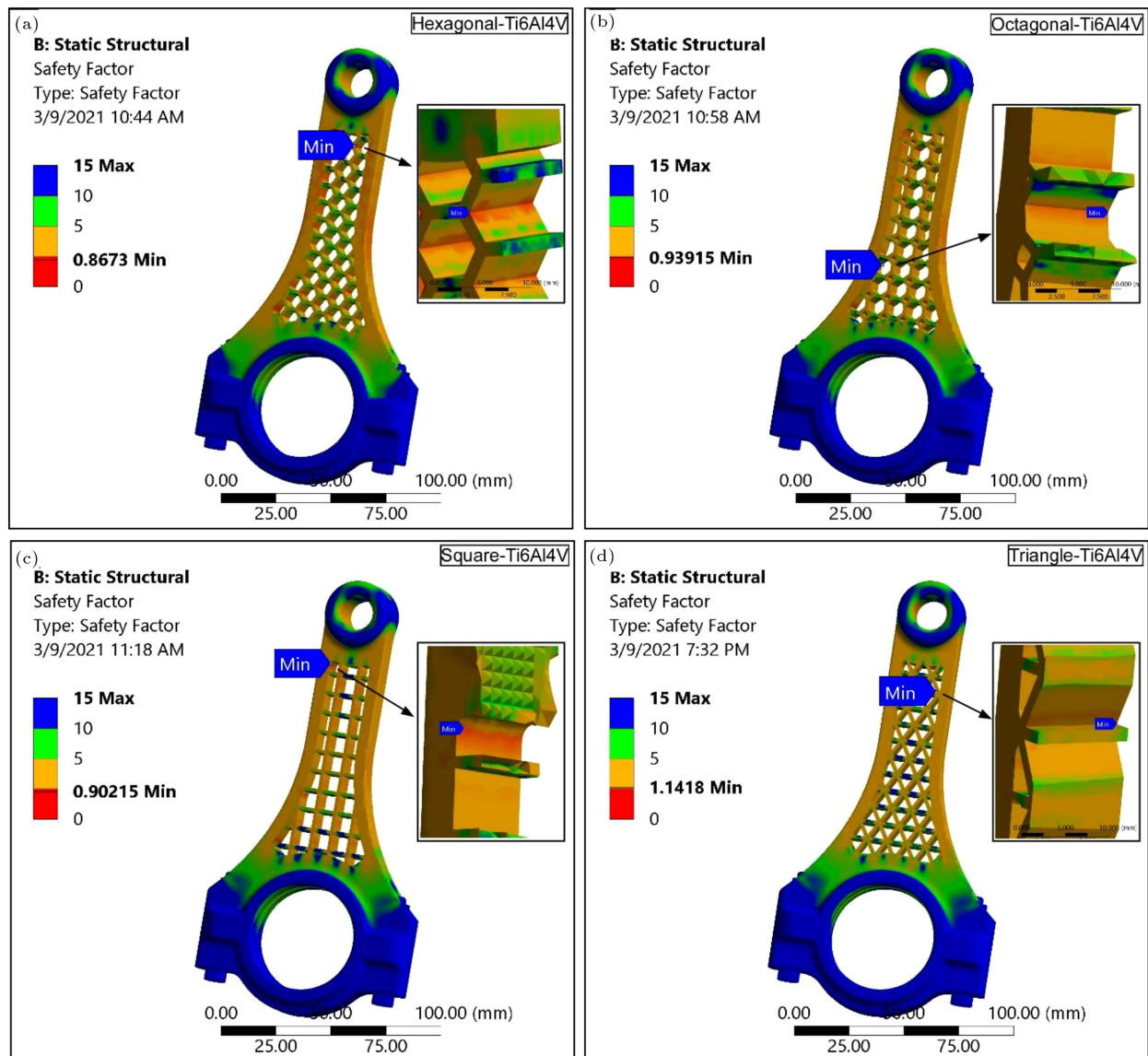


Figure 7. Cycling safety factor distributions in connecting rods with the lowest fatigue life cycle: (a) Hexagonal-Ti6Al4V, (b) octagonal-Ti6Al4V, (c) square-Ti6Al4V, and (d) triangle-Ti6Al4V.

into account. Given that increasing the thickness and chamfering at the joining corners of the lattice walls is indicative of more material input, these procedures will cause an increase in the weight of the connecting rod with lattice designs. As a general result, the triangular connecting rods meet mechanical requirements in all materials sufficiently.

4. Conclusions

In this study, different lattice designs were created on the connecting rod of an internal combustion engine. The main objective of the current research was to reduce the weight of the connecting rods without causing a significant deterioration in their mechanical properties. To this end, four different lattice designs

in hexagonal, octagonal, square, and triangular forms were made on the connecting rods and analyzed using three different materials (AISI 4140, Inconel 718, and Ti6Al4V). The load on the designed connecting rod was experimentally obtained from the engine test setup. Based on the analysis done using the finite element approach, the following results were obtained:

1. It is possible to obtain a significant reduction in weight by making lattice designs on the connecting rod body. In square, hexagonal, octagonal, and triangular cage designs, the weight was reduced by 15.75%, 14.82%, 14.48%, and 11.55%, respectively;
2. The maximum stress values of the connecting rods with lattice designs varied between 414.73 and 563.06 MPa, and these values were below the yield

stress value of the materials. Therefore, the safety factors for static conditions varied between 2.02 and 3.71. The highest safety factor belonged to the triangular design, while the lowest safety factor belonged to the hexagonal design;

3. The deformation value of the designed connecting rods changed between 0.08853 and 0.33919 mm, and the maximum deformation occurred at the Ti6Al4V material with the hexagonal lattice design;
4. Except for hexagonal, octagonal, and square designs made of Ti6Al4V material, the cycling fatigue life and cycling safety factor of all the connecting rods were above 1×10^9 cycles and 1, respectively;
5. In general, it can be claimed that the triangular connecting rods meet sufficient mechanical requirements in all materials. If AISI 4140 or Inconel 718 is chosen as the connecting rod material, all designs can be used safely.

Acknowledgment

The authors would like to thank Istanbul Technical University Information Technologies Directorate for the permission to use the software products.

References

1. Immarigeon, J.P., Holt, R.T., Koul, A.K., et al. "Lightweight materials for aircraft applications", *Mater. Charact.*, **35**(1), pp. 41–67 (1995).
2. Haber, D. "Lightweight Materials for Automotive Applications: A review", *SAE Tech. Pap.*, **2015-36-0219**, pp. 1–7 (2015).
3. Van Acker, K., Verpoest, I., De Moor, J., et al. "Lightweight materials for the automotive: Environmental impact analysis of the use of composites", *Rev. Met. Paris*, **106**(12), pp. 541–546 (2009).
4. Schöffmann, W., Beste, F., and Marquard, R. "Lightweight engine design strategies", *SAE Tech. Pap.*, **2000-01-1546**, pp. 1–7 (2000).
5. Dahotre, N.B. and Nayak, S. "Nanocoatings for engine application", *Surf. Coatings Technol.*, **194**(1), pp. 58–67 (2005).
6. Taub, A.I. and Luo, A.A. "Advanced lightweight materials and manufacturing processes for automotive applications", *MRS Bull.*, **40**(12), pp. 1045–1053 (2015).
7. Koffler, C. and Rohde-Brandenburger, K. "On the calculation of fuel savings through lightweight design in automotive life cycle assessments", *Int. J. Life Cycle Assess.*, **15**(1), pp. 128–135 (2010).
8. Maconachie, T., Leary, M., Lozanovski, B., et al. "SLM lattice structures: Properties, performance, applications and challenges", *Mater. Des.*, **183**, pp. 1–18 (2019).
9. Chu, C., Graf, G., and Rosen, D.W. "Design for additive manufacturing of cellular structures", *Comput. Aided. Des. Appl.*, **5**(5), pp. 686–696 (2008).
10. Froes, F.H. and Dutta, B. "The additive manufacturing (AM) of titanium alloys", *Adv. Mater. Res.*, **1019**, pp. 19–25 (2014).
11. Seifi, M., Salem, A., Beuth, J., et al. "Overview of materials qualification needs for metal additive manufacturing", *Jom*, **68**(3), pp. 747–764 (2016).
12. Bourell, D.L. "Perspectives on additive manufacturing", *Annu. Rev. Mater. Res.*, **46**, pp. 1–18 (2016).
13. Zhang, Y., Wu, L., Guo, X., et al. "Additive manufacturing of metallic materials: A review", *J. Mater. Eng. Perform.*, **27**(1), pp. 1–13 (2018).
14. Ashby, M.F., Evans, A.G., Fleck, N.A., et al., *Metal Foams*, 1st Ed., Elsevier, America (2000).
15. Flores, I., Kretschmar, N., Azman, A.H., et al. "Implications of lattice structures on economics and productivity of metal powder bed fusion", *Addit. Manuf.*, **31**, pp. 1–17 (2020).
16. Singh, P., Pramanik, D., and Singh, R.V. "Fatigue and structural analysis of connecting rod's material Due to (C.I) using FEA", *Int. J. Automot. Eng. Technol.*, **4**(4), pp. 245–253 (2015).
17. Baldini, A., Strozzi, A., Bertocchi, E., et al. "Stresses in the cap of a connecting rod", *Eng. Fail. Anal.*, **129**, pp. 1–15 (2021).
18. Kumar, A. and Parmar, E.S. "Analytical study and design analysis of connecting rod of mahindra pijo by finite element analysis", *Int. J. Sci. Dev. Res.*, **3**(9), pp. 114–123 (2018).
19. Ramani, H.B., Kumar, N., and Kasundra, P.M. "Analysis of connecting rod under different loading condition using Ansys software", *Int. J. Eng. Res. Technol.*, **1**(9), pp. 1–5 (2012).
20. Thakare, N.U., Bhusale, N.D., Shinde, R.P., et al. "Finite element analysis of connecting rod using Ansys", *Int. J. Adv. Sci. Eng. Technol.*, **3**(2), pp. 82–86 (2015).
21. Andoko, D. and Saputro, N.E. "Strength analysis of connecting rods with pistons using finite element method", *MATEC Web Conf.*, pp. 1–6 (2018).
22. Jia, D., Li, Y., Deng, X., et al. "Design research on forging mark of connecting rod", *Eng. Fail. Anal.*, **113**, pp. 1–9 (2020).
23. Saravanan, A., Suresh, P., Sudharsan, G., et al. "Static analysis and weight reduction of aluminum casting alloy connecting rod using finite element method", *Int. J. Mech. Prod. Eng. Res. Dev.*, **8**(3), pp. 507–518 (2018).
24. Muhammad, A., Ali, M.A.H., and Shanono, I.H. "Finite element analysis of a connecting rod in ANSYS: An overview", *IOP Conf. Ser. Mater. Sci. Eng.*, pp. 1–16 (2020).
25. Vadaverao, A.A. and Naik, S.B. "Design of connecting rod for weight reduction using alternative composite material", *Int. J. Mech. Prod. Eng. Res. Dev.*, **10**(3), pp. 12375–12394 (2020).

26. Yamagata, H. “The connecting rod”, In *The Science and Technology of Materials in Automotive Engines*, 1st Ed., Woodhead Publishing, pp. 207–227 (2005).
27. Ajayi Oluwaseun, K., Malomo, B.O., Samuel, P.D., et al. “Failure modeling for titanium alloy used in special purpose connecting rods”, *Mater. Today Proc.*, **45**(6), pp. 4390–4397 (2021).
28. Loga, P.S.R. and Ku, P.X. “Design and fatigue characteristics of connecting rod by using finite element analysis”, *AIP Conf. Proc.* (2020).
29. Rosso, S., Savio, G., Uriati, F., et al. “Optimization approaches in design for additive manufacturing”, *Proc. Int. Conf. Eng. Des. ICED, Delft*, pp. 809–818 (2019).
30. Shanmugasundar, G., Dharanidharan, M., Vishwa, D., et al. “Design, analysis and topology optimization of connecting rod”, *Mater. Today Proc.*, **46**(9), pp. 3430–3438 (2021).
31. Damon, J., Koch, R., Kaiser, D., et al. “Process development and impact of intrinsic heat treatment on the mechanical performance of selective laser melted AISI 4140”, *Addit. Manuf.*, **28**, pp. 275–284 (2019).
32. Wang, Z., Guan, K., Gao, M., et al. “The microstructure and mechanical properties of deposited-IN718 by selective laser melting”, *J. Alloys Compd.*, **513**, pp. 518–523 (2012).
33. Vrancken, B., Thijs, L., Kruth, J.P., et al. “Heat treatment of Ti6Al4V produced by selective laser melting: Microstructure and mechanical properties”, *J. Alloys Compd.*, **541**, pp. 177–185 (2012).
34. Witek, L. and Zelek, P. “Stress and failure analysis of the connecting rod of diesel engine”, *Eng. Fail. Anal.*, **97**, pp. 374–382 (2019).
35. Temizer, İ. “The combustion analysis and wear effect of biodiesel fuel used in a diesel engine”, *Fuel*, **270**, pp. 1–11 (2020).
36. Temizer, İ. and Eskici, B. “Investigation on the combustion characteristics and lubrication of biodiesel and diesel fuel used in a diesel engine”, *Fuel*, **278**, pp. 1–9 (2020).
37. Campbell, J., *Complete Casting Handbook*, Metal Casting Processes, Metallurgy, Techniques and Design, First edit, Elsevier Ltd., Brummagem, UK (2011).
38. Pan, Z. and Zhang, Y. “Numerical investigation into high cycle fatigue of aero kerosene piston engine connecting rod”, *Eng. Fail. Anal.*, **120**, pp. 1–13 (2021).
39. Ramesh, B.T., Koppad, V., and Hemantha, R.T. “Analysis and optimization of connecting rod with different materials”, *World J. Res. Rev.*, **4**(1), pp. 33–39 (2017).

Biographies

Mustafa Guven Gok graduated from Department of Metallurgical Education, Firat University with BSc and MSc degrees in 2008 and 2010, respectively. Later, he received his PhD degree from the Department of Metallurgical and Materials Engineering, Istanbul Technical University in 2015. Dr. Gok joined the Materials Science and Engineering Department of Hakkari University in 2015, and he has been working at Hakkari University since 2016. His study interests include plasma spray coating and Spark Plasma Sintering (SPS) processes, thermal barrier coatings, self-healing ceramics, biomaterials, finite element analysis, and materials of internal combustion engine.

Omer Cihan was born in 1986. He received his MSc degree in Mechanical Training of from Firat University, Elazığ, Turkey in 2011. Then, he completed his PhD program in Mechanical Engineering from Istanbul Technical University, Istanbul, Turkey in 2017. He worked as a Research Assistant at University of Istanbul Technical, Mechanical Engineering Department, Turkey from 2010 to 2017. He is currently working at Hakkari University, Turkey as an Assistant Professor. His main research interests include engine materials, friction, wear, engine testing, engine performance and emissions, engine construction, rotary engine, engine electronic control unit, and internal combustion engine.